Received: 30 June 2021 | Revised: 5 August 2021 | Accepted: 5 August 2021

DOI: 10.1002/jccs.202100267

SPECIAL ISSUE PAPER

JCCS JOURNAL OF THE CHINESE CHEMICAL SOCIETY

Photoluminescence of P3HT:PCBM bulk heterojunction thin films and effect of external electric field

Sudhakar Narra[1,2] | **Shuo-En Tsai**[1] | **Kamlesh Awasthi**[1,2] | **Shailesh Rana**[1] | **Eric Wei-Guang Diau**[1,2] | **Nobuhiro Ohta**[1,2]

[1]Department of Applied Chemistry and Institute of Molecular Science, National Yang Ming Chiao Tung University, Hsinchu, Taiwan

[2]Center for Emergent Functional Matter Science, National Yang Ming Chiao Tung University, Hsinchu, Taiwan

Correspondence
Eric Wei-Guang Diau and Nobuhiro Ohta, Department of Applied Chemistry and Institute of Molecular Science, National Yang Ming Chiao Tung University, 1001 Ta-Hseuh Road, Hsinchu 300093, Taiwan.
Email: diau@mail.nctu.edu.tw (E. W.-G. D.)
and
Email: nohta@nctu.edu.tw (N. O.)

Funding information
Ministry of Education, Taiwan, Grant/Award Number: SPROUT Project; Ministry of Science and Technology, Taiwan, Grant/Award Number: MOST 108-2113-M-009-001

Abstract

Steady-state and time-resolved photoluminescence (PL) and electro-photoluminescence (E-PL) have been recorded for bulk heterojunction samples of thin films of regio-regular poly(3-hexylthiophene) (P3HT) and methyl [6,6]-phenyl-C61-butanoate (PCBM). The PL spectra of the bulk heterojunction samples showed a monotonic decrease of PL quantum yield with increased PCBM content in the film. The PL decay was measured with both a femtosecond up-conversion technique and a time-correlated single-photon-counting technique. The mechanism of PL quenching deviated from a simple Stern-Volmer equation, explained in terms of an apparent static quenching with a *sphere-of-action* model and dynamic quenching. With increased content of PCBM, the static quenching played a dominant role. Upon application of an electric field, the E-PL spectra of both P3HT and bulk heterojunction samples showed an enhanced quantum yield and incremented lifetime of PL of P3HT. The long-range electron transfer from P3HT to PCBM was retarded upon application of an electric field; the field-induced change increased with increasing PCBM content.

KEYWORDS

bulk heterojunction, electric-field effects, FLIM, P3HT, PCBM, photoluminescence

1 | INTRODUCTION

Polymer-based organic solar cells with π-conjugation are at the forefront of organic photovoltaic research; the efficiencies of their photon conversion (PCE) attain 18% after the advent of non-fullerene-based acceptors.[1–5] The advantages of polymeric solar cells are their low cost, flexibility, designability, and slight toxicity, unlike Si-based solar cells.[1–5] A small current density and a fill factor are two challenging issues that prevent the PCE of polymeric solar cells from surpassing the theoretical limit, 20%.[1–5] To improve their device performances a thorough understanding of the mechanism of operation of the polymeric solar cell devices is necessary. As the diffusion length of excitons in the conjugated polymers is of order a few nanometers, polymeric solar cells are conventionally prepared in the form of bulk heterojunction architectures on mixing poly(3-hexylthiophene) (P3HT) and methyl [6,6]-phenyl-C61-butanoate (PCBM)[6,7]; an interfacial contact with an acceptor having a large electron mobility is thus necessary to harvest the generated excitons before recombination.[7] P3HT:PCBM bulk heterojunction samples are generally a poor choice for solar cells, but they are highly preferable for fundamental studies because much photophysical investigation has been performed using both steady-state and transient optical techniques such as ultraviolet (UV)–vis absorption, photoluminescence (PL), ultrarapid transient absorption

(vis-IR), fluorescence up-conversion and time-domain Raman spectra to understand their mode of operation.[8–24]

In a mixture of P3HT with PCBM, the absorption spectra of P3HT typically show a blue shift, broadening, and a poor absorption intensity when blend morphologies are ununiform or the conjugation length of crystalline P3HT molecules is disturbed.[5,14–16] PL quenching occurs similarly with an increased proportion of PCBM molecules.[12–14,17,18] The mechanism of this quenching was explained with a dynamic and apparently static quenching model.[12,13,18–21] The dynamic quenching model was strengthened from the PL decay measurements; Förster-type energy transfer was proposed to exist between P3HT and PCBM molecules.[18–21] Transient absorption spectra indicate a formation of excitons, charge-transfer states, polarons and their subsequent recombination dynamics of samples of mixtures.[8–10,22] Near-IR-excited transient inverse Raman spectra revealed that 70% of P3HT molecules form interfaces with PCBM molecules in 1:1 mixtures.[11]

An electric field plays a prominent role in the yield of primary charge carriers by altering photochemical paths that lead to charge-separated states across the interfaces between donors and acceptors in bulk heterojunction samples. It is thus necessary to know the effects of an electric field on the structure and dynamics of transient species such as an exciton, a radical-ion pair, and a charge-separated state. Steady-state PL experiments performed under a static electric field and a reverse bias show a quenching of fluorescence due to enhanced charge-separated states in bulk heterojunctions of a polymer.[17,25] We showed that an external electric field affects the fluorescence intensities of locally excited states of isolated donors or acceptors, and exciplexes, and thereby alters the rates of photoinduced electron transfer of methylene-linked compounds of phenanthrene and N,N-dimethylaniline, carbazole and methyl terephthalate, and push-pull-type porphyrins in a poly(methyl methacrylate) (PMMA) polymer film.[26–30] These studies of the effect of an electric field on the fluorescence of push-pull porphyrins embedded in PMMA and sensitized on TiO_2 revealed that quenching is efficient for sensitized films on TiO_2 because of a rapid injection of electrons into TiO_2.[30] Electric-field effects on the fluorescence of π-conjugated polymers such as poly[2-(phenyl)-3-(4′-(3,7-dimethyloctyloxy)phenyl)-1,4-phenylenevinylene-*co*-2-(11′-decylsulfanylundecanyloxy)-5-methoxy-1,4-phenylene vinylene] (S3-PPV) and rr-P3HT were similarly examined.[31–34] Upon application of an electric field S3-PPV showed an enhanced or quenched PL dependent on the excitation wavelength.[31] The effects of electric field on fluorescence for rr-P3HT were measured for various configurations, namely P3HT embedded in a PMMA polymer matrix, junction structures of P3HT (FTO/TiO_2/Sb_2S_3/P3HT/PMMA/Ag, FTO/TiO_2/P3HT/PMMA/Ag and FTO/P3HT/PMMA/Ag). Non-radiative processes were affected in those films, depending on the direction of the applied field in P3HT films having a junction structure,[32,34] but the effects of an electric field on the dynamics of P3HT having a bulk heterojunction with electron acceptors were not studied. In the present work, we investigated the effect of an external electric field on the PL intensity and decay of P3HT:PCBM mixture films using steady-state and time-resolved electrophotoluminescence (E-PL). An applied electric field enhanced the steady-state PL spectra of both pristine and mixture films. The transient decay of these samples measured in the presence of an applied electric field showed that long-lived excitonic states were affected by the application of that electric field. The field-induced change of electron transfer from P3HT to PCBM depended on the PCBM concentration.

2 | RESULTS AND DISCUSSION

2.1 | Absorption and PL characteristics of P3HT and P3HT:PCBM mixed films

Figure 1 shows absorption and PL spectra of P3HT, PCBM, and their mixtures. The absorption spectrum of P3HT shows a broad line with a maximum at 523 nm and a shoulder at 605 nm, associated with the weakly interacting H-aggregate states of the polymeric film[23,24]; hereafter, these lines are denoted 0–1 and 0–0, respectively. The absorption and PL maxima are consistent with the spectra of P3HT thin films. The spectrum of PCBM has maximum absorption at 338 nm with a broad tail spanning all visible and near-infrared regions. The absorption associated with P3HT composition decreased, whereas the absorption associated with the PCBM concentration increased upon increasing the ratio of PCBM content in the mixture films. The absorption spectra of mixtures resembled that of the pristine film until the percentage of PCBM by mass attained 50%. The 0–1 band of a PCBM mixture (50%) showed a blue shift from 523 nm to 486 nm, whereas the maximum corresponding to the PCBM molecule remained nearly unchanged. This effect indicates that no complexes existed between P3HT and PCBM, but the blue shift of the 0–1 line of P3HT was associated with decreased crystalline order in the polymeric chains of P3HT because of the presence of PCBM molecules.[16]

As in the case of the absorption spectrum, the PL spectrum of P3HT showed two emission lines, with maxima at 648 (G1) and 712 nm (G2), associated with weakly

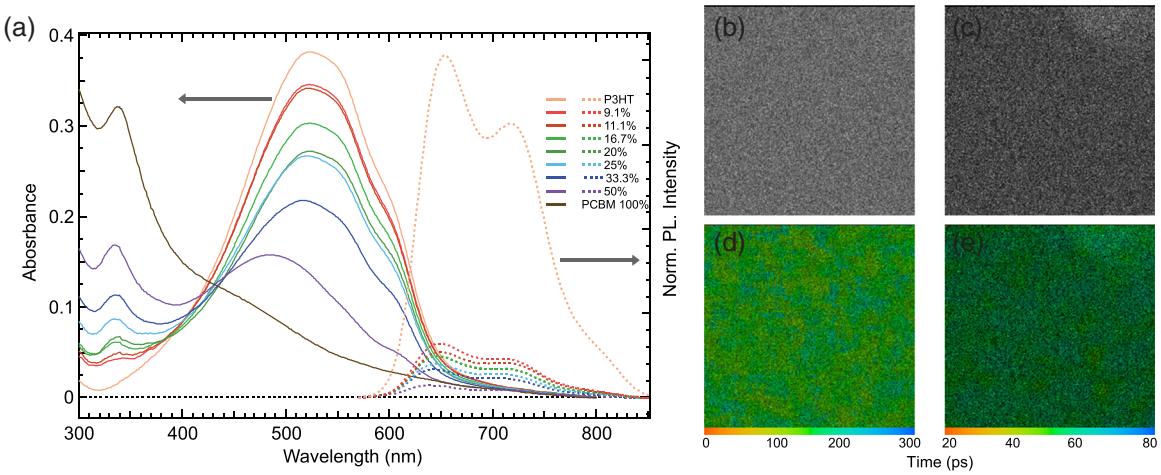

FIGURE 1 (a) UV–vis (left axis) and PL spectra (right axis) of pristine P3HT, PCBM and their mixtures. The proportion of PCBM in the mixtures, that is, PCBM/(P3HT + PCBM), was varied between 9.1 and 50%. The thin-film samples were excited at 450 nm for PL measurements. The fluorescence intensity and lifetime distribution images of P3HT (b and d) and P3HT:PCBM-50% (c and e) mixture films. The images shown here represent an area 50 × 50 μm. The thickness of the film of samples for optical measurements was ~0.5 μm

interacting H-aggregate states.[23,24] These emission maxima were blue-shifted in the mixture films. The shift of G1 and G2 bands, analogous to absorption, is associated with a decreased conjugation length of P3HT chains in the presence of PCBM.[16] The PL intensity showed a significant decrease even with a small proportion of PCBM, that is, P3HT:PCBM = 10:1 (PCBM 9.1% mixture), and thereafter a small but monotonic decrease occurred with further increased PCBM content in the mixed films. The PL spectra shown in Figure 1 were normalized to the absorption intensity of the maximum at 523 nm to make corrections as the increase of the PCBM proportion decreased the P3HT absorption for a constant thickness of the sample film. As a result, the decreased PL intensity in a mixed film shown in Figure 1 should be understood as a quenching of the P3HT fluorescence by PCBM molecules. An extended view of PL spectra of P3HT:PCBM mixed films with varied ratios is shown in Figure S1. Samples of pristine P3HT and P3HT:PCBM = 1:1 (PCBM 50%) were examined to probe aggregates with experiments involving the PL intensity and lifetime imaging. As Figure 1 shows, both pristine and mixture samples showed no aggregates at micrometer level, even at the largest PCBM proportion. An aggregation-induced quenching of fluorescence can thus be excluded in these samples.

2.2 | Mechanism of fluorescence quenching in P3HT:PCBM mixture films

The mechanism of PL quenching is understandable in terms of dynamic quenching and static quenching, even though the steady-state absorption of the mixture samples indicated no formation of a ground-state complex between P3HT and PCBM molecules for static quenching to occur. The PL decay profiles obtained at 650 nm on using femtosecond fluorescence up-conversion showed that both the PL intensity immediately after irradiation and the PL lifetimes depended on the mixing ratio between P3HT and PCBM (see Figure 2). The transient kinetic data were fitted on assuming a tri-exponential function; average lifetimes were computed with an amplitude-average lifetime. The fitted results appear in Tables S1. The assignments of the three components are torsional relaxation, exciton diffusion to low energy states (down-hill relaxation), and exciton decay from lowest emitting state for pristine P3HT sample,[32] while the sub-picosecond component involves rapid injection of electron to PCBM in the case of mixture samples. Figure 2a,b clearly indicates that the change of lifetime followed the change of PL intensity shown in Figure 1. Figure 2b shows an overlay of PL intensity and average lifetime as a function of PCBM concentration. Both steady-state PL intensity and lifetime of transient decay mutually correlated well, with minor differences that translated into various quenching scenarios, as revealed from the Stern-Volmer plots in the inset of Figure 2c. The PL lifetimes show a linear plot as a function of concentration of PCBM, as expected in the Stern-Volmer relation; the model of dynamic quenching presented in Equation (1) is applicable.[21,35]

$$\frac{\tau_0}{\tau} = \left(1 + K_q[Q]\right) \tag{1}$$

Here, τ_0 and τ are average PL lifetimes of samples in pristine P3HT and in a mixture, K_q is a collisional quenching coefficient and $[Q]$ is the concentration of a quencher, that is, PCBM.

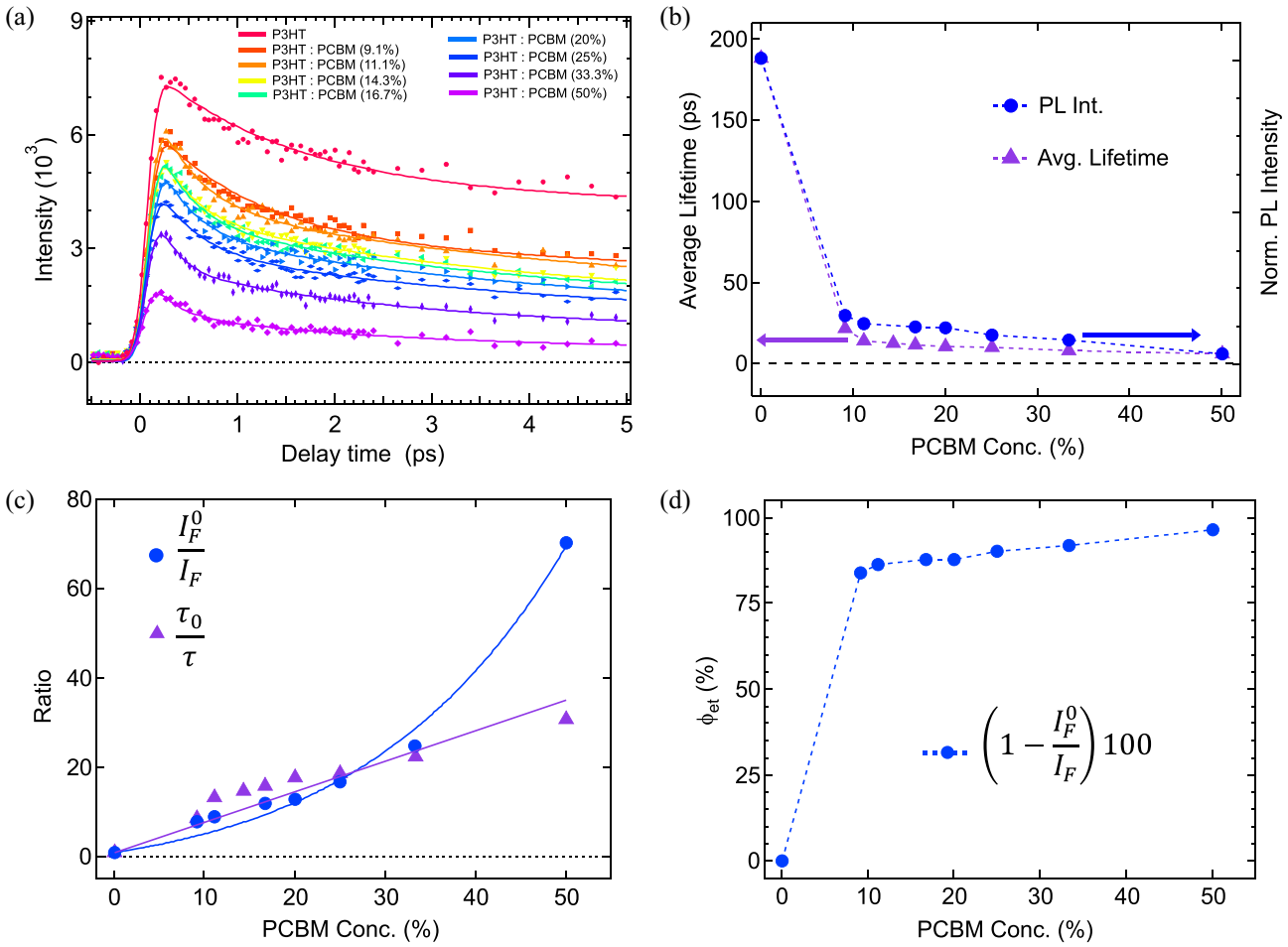

FIGURE 2 (a) Transient PL decay profiles of P3HT and P3HT:PCBM mixtures measured at 650 nm with femtosecond fluorescence up-conversion spectra. The samples were excited with a pump pulse at 400 nm; emission from samples was up-converted using a gate pulse at 800 nm. The curves fitted to the decay profiles shown here were obtained on fitting the data to a tri-exponential function. (b) Plots of PL intensity and lifetime at 650 nm as a function of PCBM concentration. (c) Plots of τ_0/τ and I_F^0/I_F obtained from emission at 650 nm as a function of PCBM concentration, with the fitted curves obtained from Equations (1) and (2), respectively. (d) Plots of efficiencies of electron transfer obtained from Equation (14) as a function of PCBM concentration

Steady-state PL intensities show a curvature, which is inexplicable based on a simple model of static or dynamic quenching. An apparent quenching known as a sphere-of-action model was hence used to fit the steady-state Stern-Volmer plots with this Equation (2).[14,35]

$$\frac{I_F^0}{I_F} = (1 + K_D[Q])\exp\left(\frac{[Q]VN}{1{,}000}\right) \quad (2)$$

Here, I_F^0 and I_F are the PL intensities in the absence and presence of quenchers, PCBM, K_D is a diffusional quenching coefficient, $V = \frac{4}{3}\pi R^3$ is the volume of the sphere of action of radius R and N is the Avogadro constant.

The steady-state PL intensities fit well to the apparent quenching model. The obtained radius of the quenching sphere of action was about 0.87 nm, which is consistent with reported value[14] 0.93 ± 0.03 nm, also near the transfer distance for P3HT,[14,36] about 1 nm. PCBM molecules lying near the quenching sphere are thus effectively quenched in a mixture sample even at a small PCBM concentration. A combination of steady-state and transient PL measurements hence uncovered the complexity of the PL quenching mode in these mixture samples.

As both static and dynamic quenching are operational in a P3HT:PCBM mixture, both effects should be considered to calculate the efficiency of electron transfer (ϕ_{et}), as described below. The electron transfer to PCBM is deemed to occur instantaneously from a hot exciton, that is, a hot excited state of P3HT, which induces static quenching; electron transfer occurs also from the emitting state of P3HT following a relaxation from the hot exciton, which induces dynamic quenching. The

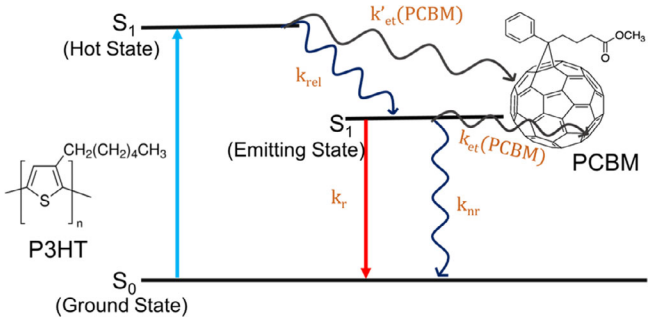

SCHEME 1 Relaxation in P3HT:PCBM mixture samples following photoexcitation: radiative process (k_r), nonradiative process (k_{nr}), relaxation (k_{rel}), electron transfer ($k'_{et}(PCBM)\&k_{et}(PCBM)$); the rate coefficient for each process is shown in parentheses

relaxation of excitons and electron transfer to PCBM are shown in Scheme 1. In the absence of static quenching, an instantaneous electron transfer to PCBM became negligible. All hot excitons created in P3HT were then considered to relax to the lowest emitting state. In such a case, the quantum yield of PL (ϕ_F) is given by Equation (3).

$$\phi_F = \frac{k_r}{(k_r + k_{nr} + k_{et}(PCBM))}; \tau = \frac{1}{(k_r + k_{nr} + k_{et}(PCBM))} \tag{3}$$

Here, k_r, k_{nr} and $k_{et}(PCBM)$ are the radiative, nonradiative and electron-transfer rate constants; τ is the PL lifetime of a P3HT:PCBM mixture. The PL quantum yield (ϕ_F) in the absence of PCBM is given by Equation (4). When PCBM is absent, $k_{et}(PCBM) = 0$; then $\phi_F \to \phi_F^0$ and $\tau \to \tau_0$.

$$\phi_F^0 = \frac{k_r}{(k_r + k_{nr})}; \tau_0 = \frac{1}{(k_r + k_{nr})} \tag{4}$$

The efficiency of electron transfer (ϕ_{et}) to PCBM is defined as

$$\phi_{et} = \frac{k_{et}(PCBM)}{(k_r + k_{nr} + k_{et}(PCBM))} = 1 - \frac{k_r + k_{nr}}{(k_r + k_{nr} + k_{et}(PCBM))} \tag{5}$$

$$\phi_{et} = 1 - \frac{\tau}{\tau_0} = 1 - \frac{\phi_F}{\phi_F^0} \tag{6}$$

ϕ_{et} given by Equation (6) is applicable in the case of dynamic quenching alone. In the present case, static quenching also causes electron transfer; ϕ_F is given by Equation (7) instead of Equation (3).

$$\phi_F = \left(\frac{k_{rel}}{k_{rel} + k'_{et}(PCBM)}\right)\left(\frac{k_r}{k_r + k_{nr} + k_{et}(PCBM)}\right); \quad \tau = \frac{1}{(k_r + k_{nr} + k_{et}(PCBM))} \tag{7}$$

Here, k_{rel} and $k'_{et}(PCBM)$ are the rate constant of the relaxation from photoexcited state to the emitting state and the rate constant of the electron transfer from the photoexcited state to PCBM, which gives static quenching, respectively. Then, ϕ_{et} in the presence of static quenching is defined as

$$\begin{aligned}\phi_{et} &= \left(\frac{k'_{et}(PCBM)}{k_{rel} + k'_{et}(PCBM)}\right) + \left(\frac{k_{et}(PCBM)}{k_r + k_{nr} + k_{et}(PCBM)}\right)\left(\frac{k_{rel}}{k_{rel} + k'_{et}(PCBM)}\right) \\ &= \left(1 - \frac{k_{rel})}{k_{rel} + k'_{et}(PCBM)}\right) + \left(1 - \frac{k_r + k_{nr}}{k_r + k_{nr} + k_{et}(PCBM)}\right)\left(\frac{k_{rel}}{k_{rel} + k'_{et}(PCBM)}\right)\end{aligned} \tag{8}$$

The ratio of the PL quantum yields is given as

$$\frac{\phi_F}{\phi_F^0} = \left(\frac{k_{rel}}{k_{rel} + k'_{et}(PCBM)}\right)\left(\frac{k_r + k_{nr}}{k_r + k_{nr} + k_{et}(PCBM)}\right) \tag{9}$$

$$\left(\frac{\phi_F}{\phi_F^0}\right)\left(\frac{\tau_0}{\tau}\right) = \left(\frac{k_{rel}}{k_{rel} + k'_{et}(PCBM)}\right) \tag{10}$$

On substituting Equations (4), (7) and (10) into Equation (8), ϕ_{et} becomes

$$\phi_{et} = \left(1 - \frac{\phi_F}{\phi_F^0}\right) \tag{11}$$

Equation (11) indicates that the efficiency of electron transfer is determined by the ratio of PL intensities even when both static and dynamic quenching exist. The intensity ratio, that is $\frac{I_F}{I_F^0}$, can replace $\frac{\phi_F}{\phi_F^0}$. The value of ϕ_{et} shown in Figure 2d displays an increased efficiency even at small PCBM concentrations; ϕ_{et} approached 90% when the PCBM concentration in the film attained 50%. The difference between the plots of τ_0/τ and of $I_F{}^0/I_F$ as a function of PCBM concentration became more significant with increasing PCBM concentration, as shown in

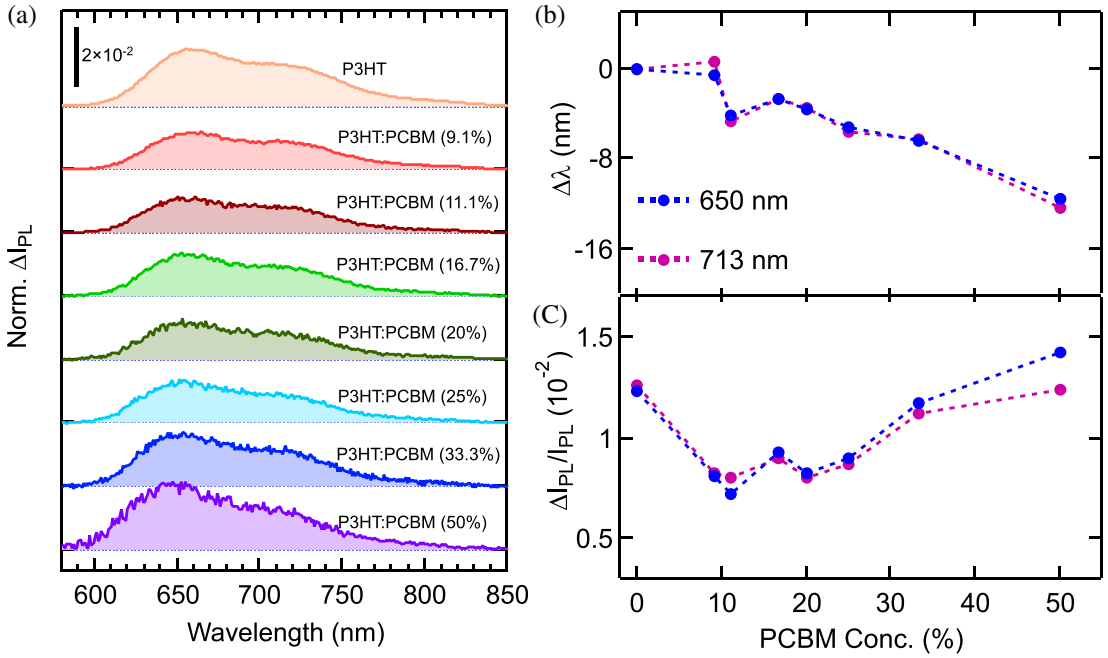

FIGURE 3 (a) E-PL spectra recorded at the second harmonic of the modulation of an applied electric field of strength 0.3 MV/cm for P3HT and P3HT:PCBM mixtures. The intensity is normalized with respect to the steady-state PL maximum intensity at 650 nm. The samples were excited at 450 nm. The proportion of PCBM in each mixture is indicated in parentheses; (b) shift of maximum of P3HT:PCBM samples relative to the maximum of P3HT, that is, 650 and 713 nm, respectively, (c) plots of $\Delta I_{PL}/I_{PL}$ of P3HT:PCBM samples as a function of PCBM content (mass %)

Figure 2c, indicating that static quenching became more efficient with increasing concentration of PCBM.

2.3 | Effect of an electric field on the PL spectrum and decay

The effects of an external electric field on the exciton dissociation and charge transfer to PCBM molecules were investigated on monitoring the field-induced change of PL intensity and decay profiles of pure P3HT and P3HT:PCBM mixture samples, which were prepared as sandwich structures in the form of ITO/SiO_2/active-layer/LiF/Ag. When an external electric field was applied to the isotropic samples, an altered intensity of the PL spectrum, a shift or broadening of the spectral lines were induced.[27] The spectral shift and broadening were caused by a change of polarizability and electric dipole moment, respectively, between the emitting state and the ground state. To understand which processes are dominant in the observed E-PL spectra, the observed E-PL spectra are generally fitted with a linear combination of zeroth, first, and second derivatives of the PL spectrum. In the present case, E-PL spectra were recorded at the second harmonic of the modulation frequency of the applied electric field of strength 0.3 MV/cm for pure P3HT and P3HT:PCBM mixture samples; the results appear in Figures 3a. The excitation wavelength for E-PL and PL experiments was 450 nm, at which the effect of the field on the absorption intensity was negligible (Figure S2). The field-induced change of the PL intensity (ΔI_{PL}) observed was ascribed to the quadratic-field effects on the PL as the signal intensity ΔI_{PL} is proportional to the square of the applied field strength, as shown in Figure S3. The E-PL spectra shown in Figure 3a, of which the shapes are similar to the PL spectra, indicated that the PL intensity increased in the presence of an applied electric field of order 10^{-2} for both G1 and G2 bands of all samples. The E-PL spectra were fitted with two Gaussian lines, G1 and G2, derived from the steady-state PL spectra (Figure S4). G1 and G2 lines in PL spectra and E-PL spectra showed a blue shift with increasing content of PCBM (see Figure 3b). The ratio of ΔI_{PL} and PL intensity (I_{PL}), $\Delta I_{PL}/I_{PL}$, estimated for G1 and G2 lines, is plotted as a function of PCBM content (see Figure 3c). The magnitudes of $\Delta I_{PL}/I_{PL}$, evaluated for G1 and G2 lines of P3HT are similar; $\frac{\Delta I_{PL}}{I_{PL}}$ ~0.012. This value is slightly smaller than that estimated earlier,[32,34] which might be due to the difference of P3HT sample morphology or conditions of device preparation.

The electric-field effects on the PL decay profiles were examined for these samples—pristine P3HT, 9.1, 16.7 and 33.3% mixtures, that is, P3HT:PCBM = 10:1, 5:1 and 1:1, using a laboratory-built time-resolved E-PL measurement system capable of detecting precisely a small

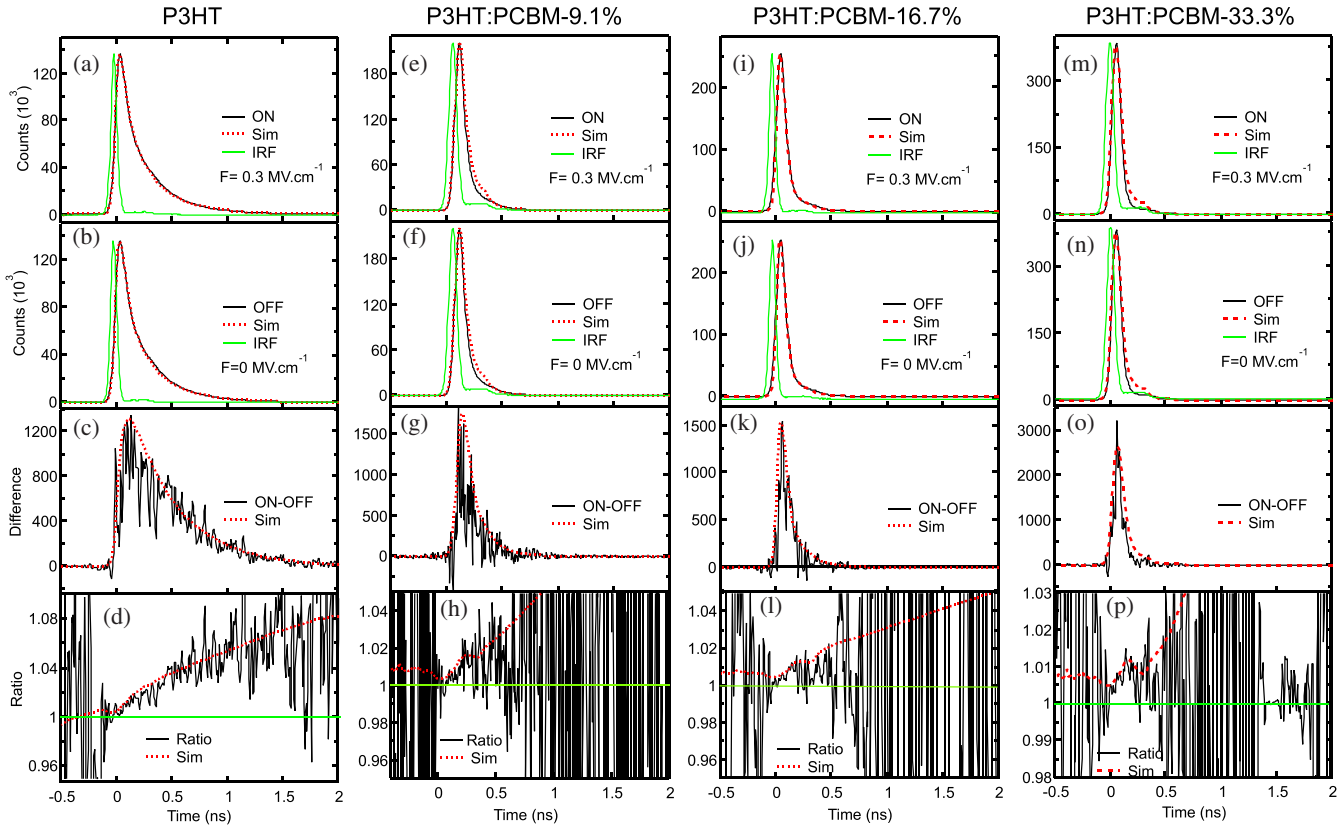

FIGURE 4 Effects of external electric field on PL decay profiles of P3HT and P3HT:PCBM mixtures with PCBM proportions 9.1, 16.7 and 33.3%, respectively (from left to right). Panels (a, e, i, m) represent PL decay profiles observed in the presence of field 0.3 MV/cm ($I(t)_{ON}$) and simulated decays. Panels (b, f, j, n) represent PL decay profiles observed at zero field ($I(t)_{OFF}$) and simulated decays. Panels (c, g, k, o) represent the difference between the two decay profiles, that is, $I(t)_{ON} - I(t)_{OFF}$, and simulated curves. Panels (d, h, l, p) represent the ratio between two decay profiles, that is, $I(t)_{ON}/I(t)_{OFF}$ and simulated curves. Simulations are given by red lines

field-induced change of the decay profile.[37] Time-resolved E-PL measurements are instrumental in disentangling the processes affected by an applied electric field.[31–34,37] As the strength of applied field and wavelength of excitation in the PL decay measurements were similar to those in the steady-state PL and E-PL measurements, the results correlated with each other. PL decay profiles were measured with field strengths 0 and 0.3 MV/cm; the results appear in Figure 4, with the difference and ratio between these two decay profiles. The plots of the difference shown in Figure 4c,g,k,o clearly show a field-induced enhancement of PL intensity upon applying an external electric field, similar to the results of the steady-state E-PL spectra. The ratio plots shown in Figure 4d,h,l,p indicate that the effects of the electric field were manifested on the slowly decaying components rather than the rapidly decaying components. The PL decay profiles measured with fields 0 and 0.3 MV/cm, as well as the difference and ratio between these decays, were simulated on assuming a bi-exponential function; the results appear in Figure 4 and Table 1. The assignments of the time constants in Table 1 are similar to the τ_2 and τ_3 of Table S1. The difference in the lifetime values between fluorescence up-conversion and time-correlated single-photon-counting (TCSPC) techniques are due to the differences in the morphologies of the sample prepared on glass and SiO_2 substrates. An applied electric field on both P3HT and P3HT:PCBM mixture samples decreased the rate of PL decay, which is explicable in terms of the field-induced deceleration of non-radiative processes, including electron transfer from P3HT to PCBM.

A field-induced enhancement of PL intensity and a field-induced increase of PL lifetime were associated with a field-induced increase of ϕ_F due to altered k_{nr}, k_{et}, and k'_{et} in Scheme 1. As the electric-field effect was observed in pristine P3HT, that is, without PCBM, a field-induced change of k_{nr} must be considered. ϕ_F at zero field is given in Equation (7), whereas, upon application of an electric field, $\phi_F + \Delta\phi_F$ is given in Equation (12),

$$\phi_F + \Delta\phi_F = \left(\frac{k_{rel}}{k_{rel} + k'_{et}(PCBM) + \Delta k'_{et}(PCBM)}\right)\left(\frac{k_r}{k_r + k_{nr} + \Delta k_{nr} + k_{et}(PCBM) + \Delta k_{et}(PCBM)}\right) \quad (12)$$

Here, $\Delta\phi_F$, Δk_{nr}, $\Delta k_{et}(PCBM)$, and $\Delta k'_{et}(PCBM)$ are the field induced changes in ϕ_F, k_{nr}, $k_{et}(PCBM)$, and $k'_{et}(PCBM)$, respectively. In Figure 4, $I(t)_{ON}/I(t)_{OFF}$ is nearly unity at time $t = 0$, indicating that the PL intensity immediately following a photoexcitation was unaffected by an applied electric field; the population of the emitting state following photoexcitation was unaffected by an applied electric field. In such a case, $\Delta k'_{et}(PCBM)$ became negligible; $\phi_F + \Delta\phi_F$ is given by Equation (13),

$$\phi_F + \Delta\phi_F = \left(\frac{k_{rel}}{k_{rel} + k'_{et}(PCBM)}\right)\left(\frac{k_r}{k_r + k_{nr} + \Delta k_{nr} + k_{et}(PCBM) + \Delta k_{et}(PCBM)}\right) \quad (13)$$

From Equations (7) and (13),

$$\Delta k_{nr} + \Delta k_{et}(PCBM) = -\frac{\left(\frac{\Delta\phi_F}{\phi_F}\right)}{\left[\left\{1 + \left(\frac{\Delta\phi_F}{\phi_F}\right)\right\}\tau\right]} \quad (14)$$

$\frac{\Delta\phi_F}{\phi_F}$, which can be estimated as $\frac{\Delta I_F}{I_F}$, was determined from the E-PL measurements. $\Delta k_{nr} + \Delta k_{et}(PCBM)$ was determined using the average PL lifetimes shown in Table 1, which were obtained with a device structure the same as that used for E-PL measurements, as the PL lifetime is sensitive to the substrate. As a function of PCBM content the values of $\Delta k_{nr} + \Delta k_{et}(PCBM)$, which are of order $10^8\,s^{-1}$, are shown in Figure 5. On assuming that the magnitude of Δk_{nr} estimated from the data for P3HT (without PCBM) is the same in a P3HT:PCBM mixed sample, $\Delta k_{et}(PCBM)$ is determined to be -9.4×10^7, -1.8×10^8, $-2.8 \times 10^8\,s^{-1}$ for P3HT:PCBM mixed samples with PCBM content 9.1, 16.7 and 33.3%, respectively.

The decreased Δk_{et} values in the mixture samples might be due to a field-induced change in the activation barrier for electron transfer. Values of Δk_{et} estimated here show an effective linearity in retarding the electron transfer upon increasing the PCBM concentration. As reported,[27,38] the effect of an electric field on the rate of photoinduced electron transfer depends strongly on the donor-acceptor distance. Even in the same pair of donor

TABLE 1 Results of simulation of PL decay profiles of P3HT and P3HT:PCBM mixture samples with PCBM proportions 9.1, 16.7, and 33.3%, respectively

Sample	F/MV/cm	τ_1/ps (A_1)	τ_2/ps (A_2)	τ^{ave}/ps ($\sum_{i=1}^{n} A_i$)
P3HT	0.3	91.2 (0.686)	340.6 (0.316)	186.3 (1.0025)
	0	90.4 (0.689)	336.5 (0.311)	166.8 (1.0000)
P3HT:PCBM (9.1%)	0.3	41.5 (0.832)	124.9 (0.169)	55.6 (1.0021)
	0	41.1 (0.831)	123.9 (0.169)	55.1 (1.0000)
P3HT:PCBM (16.7%)	0.3	39.4 (0.944)	150.8 (0.060)	46.1 (1.0040)
	0	39.2 (0.940)	150.4 (0.059)	45.9 (1.0000)
P3HT:PCBM (33.3%)	0.3	37.1 (0.966)	130.4 (0.039)	40.8 (1.0044)
	0	36.9 (0.961)	130.0 (0.038)	40.5 (1.0000)

Note: Lifetime (τ_i) and pre-exponential factor (A_1, A_2, given in parentheses) of each decay component of PL observed in the presence of an electric field (**F**) of strength 0.3 MV/cm and at zero field are shown. The average lifetime (τ_{ave}) in each decay profile is also shown. The sum of the pre-exponential factors is normalized to unity for the decay profile at zero field. The PL was monitored at wavelength $\lambda = 650$ nm.

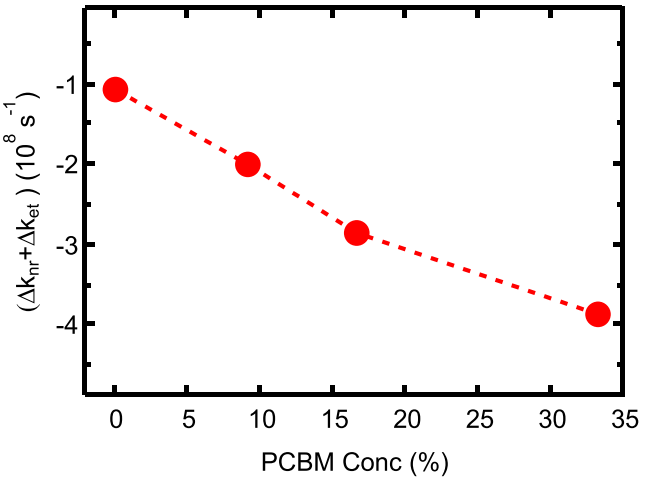

FIGURE 5 Field-induced change of $k_{nr} + k_{et}$, that is, $\Delta k_{nr} + \Delta k_{et}$, of P3HT:PCBM mixture samples obtained at field strength 0.3 MV/cm

and acceptor molecules, electron transfer was theoretically shown to be accelerated and decelerated on application of an electric field, depending on the donor-acceptor distance.[39] The present results in which the effect of electric field depends on the ratio between P3HT and PCBM in mixtures might also arise from the dependence on the donor-acceptor distance of the effect of an electric field on an electron transfer. The present results were obtained with an applied electric field, but a local field exists at the interfaces between P3HT and PCBM molecules, which might play an adverse role and retard the transport of electrons to the acceptor.

3 | EXPERIMENTS

3.1 | Sample preparation

The chemical substances in this work were purchased as follows: poly (3-hexylthiophene-2,5-diyl) (simply called P3HT), MM = 22 kDa, regioregularity 89–94%, electronic grade (Rieke Metals); methyl [6,6]-phenyl-C_{61}-butanoate (simply called PCBM), MM = 910.9 Da, purity: 99.5% (UniRegion Bio-Tech); chlorobenzene anhydrous, 99.8%, MW = 112.56 Da (Sigma-Aldrich); lithium fluoride (LiF), 98.5%, −325 mesh powder (Alfa Aesar), solid silver, 99.999% purity for deposition on a sample (Po Hsuan Enterprises); SiO_2-coated substrate in a device (Techno Print); colloidal silver (Ted Pella).

Solutions of P3HT and PCBM precursors were prepared on dissolving 15 mg/ml (m/v) in chlorobenzene as solvent. The solutions were stirred for 30 hr with magnetic stirring bars to increase the solubility of solutes. The precursor solutions were filtered with a microfilter to remove undissolved particles after prolonged stirring. P3HT:PCBM mixture solutions were prepared on intermixing appropriate aliquots of the prepared P3HT and PCBM solutions.

The SiO_2 substrates were carefully cleaned to remove surface contaminants and dust particles before spin coating and were dried in an oven about 2 hr. The cleaning of the substrates involved gently rubbing the surface of the wet substrates with a soft sponge dipped in a surfactant (Extran MA 02, Merck, detergent) under flowing tap water, followed by sonicating the substrate for 30 min in a mixture of 99.5% acetone, isopropanol, and deionized water in ratio 1:1:1. The sonicated substrates were further rinsed with deionized water and partially dried with a stream of dry N_2 gas. The dried substrates were ozonized for 10 min under intense UV light.

Thin films of P3HT, PCBM, and P3HT:PCBM mixtures were prepared with a spin-coating technique on UV-ozone-treated, well cleaned, and oven-dried SiO_2 substrates. A substrate placed on the spin coater was loaded with a prepared precursor solution and spun at rate 1,500 rpm for about 30 s and was further accelerated to 2,000 rpm for 30 s. The spin coating was performed in a glove box maintained under a steady flow of dry N_2 gas with minuscule concentrations of water vapor and oxygen. The thin films were further dried near 298 K inside the glove box.

A layer ~10 nm of LiF insulator was deposited on top of the precoated P3HT or P3HT:PCBM active layer with a thermal evaporation system operated under vacuum conditions. LiF powder was placed in a tungsten boat of an evaporation system to deposit a LiF film on top of an active layer to prevent a short circuit between the electrodes.

A silver film was deposited on top of the LiF film using a vapor deposition system operated in vacuum conditions. To apply an electric field the prepared device was connected to an external voltage source. The device prepared had an architecture of form quartz/ITO/SiO_2/P3HT:PCBM/LiF/Ag. ITO and Ag served as electrodes, SiO_2 and LiF served as insulators, P3HT:PCBM was the active layer; quartz acted as a support substrate for a device.

3.2 | Optical measurements

The UV–vis absorption spectra were recorded on a spectrophotometer (JASCO-V780) equipped with an integrating-sphere accessory (ISN-9011, JASCO). The transmittance and reflectance of thin-film samples and blank substrates were measured; the absorbance of samples was calculated after correcting for substrate losses.

The PL spectra of the samples were recorded with a fluorescence spectrometer (JASCO FP-6300). The samples were excited at 450 nm; emission from the sample was collected at 90° to the direction of propagation of the excitation light. The thin film was placed near 45° with respect to the excitation light. The slit widths of the excitation and emission monochromators were 5 and 10 nm, respectively. The emission spectra were recorded in wavelength range 570 to 850 nm. The scattering from the excitation light source was blocked with a 560-nm long-pass color glass filter in the path of the collection geometry. Transient PL decay profiles at emission wavelength 650 nm were measured using a femtosecond fluorescence up-conversion spectrometer (FOG 100, CDP systems). The thin-film samples cast on glass substrates were excited with a 150-fs laser pulse at 400 nm, obtained on doubling the fundamental of a Femtosecond Ti:Sapphire Oscillator (Chameleon, Coherent Inc.); the gate pulse was set to 800 nm. The decay profiles were obtained on measuring the up-converted signal intensity at varied intervals between emitted signal and gate pulses.

The E-A spectrum of the P3HT sample was measured with a spectrometer (Jasco EMV-100); the details were reported.[26,31] Briefly, a sinusoidal ac voltage (frequency 1 kHz) generated by a function generator (SG-4311, Iwatsu) and further amplified with a high-voltage amplifier was applied to a P3HT thin sample. The field-induced change of absorption intensity was detected with a lock-in amplifier (SR830, SRS) at the second harmonic of the modulation frequency of the applied electric field.

The E-PL spectra of P3HT, PCBM and P3HT:PCBM mixture samples were recorded, with PL spectra, with a spectrometer (FP-6300). The experimental setup for the E-PL measurement was similar to that for the steady-state PL measurement except that an electric field was applied to the samples to obtain the field-induced change of PL intensity. The experimental procedure to apply an electric field to a sample was similar to that for E-A measurements. The excitation wavelength for the E-PL measurements was chosen to be the position at which the field-induced change in absorbance was negligible.

The time-resolved E-PL measurement system used in these experiments was constructed on combining a TCSPC module to measure PL decay profiles and a modulated electric field to apply a bias to the sample; details of the system appear elsewhere.[31,37] The samples were excited with a laser pulse at 450 nm generated from the second harmonic of the femtosecond Ti:Sapphire laser (Tsunami, Spectra Physics) pumped with a diode laser (Millenia Xs, Spectra Physics). The emission from the sample was dispersed into a spectrometer (G-250 Nikon) and detected with an MCP-PMT detector (R-3809U-52, Hamamatsu). The decay profiles were obtained with a multichannel pulse analyzer (MCA). The measurement system was combined with TCSPC and a microchannel-plate photomultiplier. The field-induced changes in the decay profile were obtained with a modulated square-wave electric-pulse train consisting of positive, zero, negative, and zero voltage bias signals. The MCA channels were segmented based on the applied bias voltages; the decay profiles corresponding to the applied bias voltages were separately stored and analyzed to obtain the field-induced decay profiles and to retrieve the small changes associated with the applied field.

Experiments for fluorescence lifetime imaging were performed with a FLIM system.[40] A FLIM system comprises an inverted microscope (C1; Nikon, TE2000-E), a mode-locked Ti-Sapphire laser system (Tsunami; Spectra Physics) and a TCSPC module (SPC 830; Becker and Hickel GmbH). A microscope was used for optical imaging; a Ti-sapphire laser served for excitation; the TCSPC module provided the emission decay profiles. The imaging experiments were performed on focusing an excitation laser (Tsunami) pulse (450 nm) through a water-immersion objective (60×/1.27 NA) onto a sample; emission was collected in a back-scattering geometry followed by scanning the illuminated areas of the samples using a Galvano scanner. The excitation light was filtered from collected emission with a long-pass filter. The collected data were analyzed using software (SPCM version 9.83).

4 | CONCLUSIONS

Steady-state PL and E-PL spectra, and absorption spectra, were recorded for P3HT:PCBM bulk heterojunction thin films, with varied mixing ratios. Time-resolved decay profiles of PL and E-PL intensities were also measured. The absorption spectra showed no significant change with increasing PCBM content, indicating no complex formation between P3HT and PCBM. PL intensity and lifetime-imaging experiments performed with micrometer-level resolution also revealed no aggregate in the bulk heterojunction samples. The quantum yield of PL of P3HT decreased markedly with mixed PCBM; the magnitude of the decrease increased upon increasing the PCBM content in the bulk heterojunction samples. Transient PL decay measurements with the fluorescence up-conversion technique indicated that the PL lifetime altered greatly upon adding PCBM at a small proportion; the change was moderated after further increased PCBM content. The PL quenching mechanism was explained in terms of an apparent static quenching (known as quenching by a sphere of action) and dynamic quenching, based on the dependence of intensity and lifetime of PL of P3HT on PCBM content. Static quenching is suggested to become

dominant with increasing PCBM content. Application of an electric field to P3HT and P3HT:PCBM blended films with a bulk heterojunction induce an enhanced PL intensity and incremented PL lifetimes, because of a retardation of nonradiative processes upon application of an electric field. The field-induced change in the rate of electron transfer decreased monotonically with increasing concentration of PCBM, which likely arises from a dependence of the effect of electric field on electron transfer on the donor-acceptor distance.

ACKNOWLEDGMENTS

N. Ohta thanks Prof. Y.-P. Lee, who celebrates his 70th birthday on this occasion, and Prof. C.-S. Hsu at DAC, NYCU, for their strong support. Taiwan Ministry of Science and Technology (MOST 108-2113-M-009-001) and Center for Emergent Functional Matter Science of NYCU from The Featured Areas Research Center Program within the framework of the Higher Education Sprout Project by Taiwan Ministry of Education (MOE) supported this work.

REFERENCES

[1] G. Zhang, J. Zhao, P. C. Y. Chow, K. Jiang, J. Zhang, Z. Zhu, J. Zhang, F. Huang, H. Yan, *Chem. Rev.* **2018**, *118*, 3447.
[2] A. Karki, A. J. Gillett, R. H. Friend, T. Nguyen, *Adv. Energy Mater.* **2021**, *11*, 2003441.
[3] G. Wang, F. S. Melkonyan, A. Facchetti, T. J. Marks, *Angew. Chem. Int. Ed.* **2019**, *58*, 4129.
[4] C. Lee, S. Lee, G.-U. Kim, W. Lee, B. J. Kim, *Chem. Rev.* **2019**, *119*, 8028.
[5] Y. L. Lin, M. A. Fusella, B. P. Rand, *Adv. Energy Mater.* **2018**, *8*, 1702816.
[6] J.-L. Brédas, J. E. Norton, J. Cornil, V. Coropceanu, *Acc. Chem. Res.* **2009**, *42*, 1691.
[7] P. R. Berger, M. Kim, *J. Renew. Sustain. Energy* **2018**, *10*, 013508.
[8] H. Ohkita, S. Cook, Y. Astuti, W. Duffy, S. Tierney, W. Zhang, M. Heeney, I. McCulloch, J. Nelson, D. D. C. Bradley, J. R. Durrant, *J. Am. Chem. Soc.* **2008**, *130*, 3030.
[9] J. Guo, H. Ohkita, H. Benten, S. Ito, *J. Am. Chem. Soc.* **2010**, *132*, 6154.
[10] M. Hallermann, I. Kriegel, E. D. Como, J. M. Berger, E. von Hauff, J. Feldmann, *Adv. Funct. Mater.* **2009**, *19*, 3662.
[11] T. Takaya, I. Enokida, Y. Furukawa, K. Iwata, *Molecules* **2019**, *24*, 431.
[12] Y. Xie, Y. Li, L. Xiao, Q. Qiao, R. Dhakal, Z. Zhang, Q. Gong, D. Galipeau, X. Yan, *J. Phys. Chem. C* **2010**, *114*, 14590.
[13] S. Trotzky, T. Hoyer, W. Tuszynski, C. Lienau, J. Parisi, *J. Phys. D Appl. Phys.* **2009**, *42*, 055105.
[14] S. Engmann, V. Turkovic, P. Denner, H. Hoppe, G. Gobsch, *J. Polym. Sci. B Polym. Phys.* **2012**, *50*, 1363.
[15] Y. Kim, S. A. Choulis, J. Nelson, D. D. C. Bradley, S. Cook, J. R. Durrant, *J. Mater. Sci.* **2005**, *40*, 1371.
[16] C. Liu, W. Tseng, C. Cheng, C. Wu, P. Chou, S. Tung, *J. Polym. Sci. B Polym. Phys.* **2016**, *54*, 975.
[17] A. Gonzalez-Rabade, A. C. Morteani, R. H. Friend, *Adv. Mater.* **2009**, *21*, 3924.
[18] K. Feron, W. J. Belcher, C. J. Fell, P. C. Dastoor, *Int. J. Mol. Sci.* **2012**, *13*, 17019.
[19] W.-L. Xu, B. Wu, F. Zheng, X.-Y. Yang, H.-D. Jin, F. Zhu, X.-T. Hao, *J. Phys. Chem. C* **2015**, *119*, 21913.
[20] Y.-X. Liu, M. A. Summers, S. R. Scully, M. D. McGehee, *J. Appl. Phys.* **2006**, *99*, 093521.
[21] A. R. S. Kandada, G. Grancini, A. Petrozza, S. Perissinotto, D. Fazzi, S. S. K. Raavi, G. Lanzani, *Sci. Rep.* **2013**, *3*, 2073.
[22] S. M. Falke, C. A. Rozzi, D. Brida, M. Maiuri, M. Amato, E. Sommer, A. D. Sio, A. Rubio, G. Cerullo, E. Molinari, C. Lienau, *Science* **2014**, *344*, 1001.
[23] J. Clark, C. Silva, R. H. Friend, F. C. Spano, *Phys. Rev. Lett.* **2007**, *98*, 206406.
[24] F. C. Spano, *Acc. Chem. Res.* **2010**, *43*, 429.
[25] A. Weu, T. R. Hopper, V. Lami, J. A. Kreß, A. A. Bakulin, Y. Vaynzof, *Chem. Mater.* **2018**, *30*, 2660.
[26] S. Umeuchi, Y. Nishimura, I. Yamazaki, H. Murakami, M. Yamashita, N. Ohta, *Thin Solid Films* **1997**, *311*, 239.
[27] N. Ohta, *Bull. Chem. Soc. Jpn.* **2002**, *75*, 1637.
[28] H. Kawabata, Y. Nishimura, I. Yamazaki, K. Iwai, N. Ohta, *J. Phys. Chem.* **2001**, *105*, 10261.
[29] N. Ohta, M. Koizumi, S. Umeuchi, Y. Nishimura, I. Yamazaki, *J. Phys. Chem.* **1996**, *100*, 16466.
[30] H.-Y. Hsu, H.-C. Chiang, J.-Y. Hu, K. Awasthi, C.-L. Mai, C.-Y. Yeh, N. Ohta, E. W.-G. Diau, *J. Phys. Chem. C* **2013**, *117*, 24761.
[31] T. Iimori, K. Awasthi, C.-S. Chiou, E. W.-G. Diau, N. Ohta, *ACS Appl. Energy Mater.* **2018**, *1*, 6136.
[32] T. Iimori, K. Awasthi, C.-S. Chiou, E. W.-G. Diau, N. Ohta, *Phys. Chem. Chem. Phys.* **2019**, *21*, 5695.
[33] K. Awasthi, C.-S. Chiou, T. Iimori, E. W.-G. Diau, N. Ohta, *J. Phys. Chem. C* **2019**, *123*, 12647.
[34] M. S. Mehata, C.-S. Hsu, Y.-P. Lee, N. Ohta, *J. Phys. Chem. B* **2010**, *114*, 6258.
[35] J. R. Lakowicz, *Principles of fluorescence spectroscopy*, Springer, Boston, MA **2006**.
[36] M. Theander, A. Yartsev, D. Zigmantas, V. Sundström, W. Mammo, M. R. Andersson, O. Inganäs, *Phys. Rev. B* **2000**, *61*, 12957.
[37] M. Tsushima, T. Ushizaka, N. Ohta, *Rev. Sci. Instrum.* **2004**, *75*, 479.
[38] T. Ito, I. Yamazaki, N. Ohta, *J. Phys. Chem. B* **2002**, *106*, 895.
[39] M. Hilczer, M. Tachiya, *J. Chem. Phys.* **2002**, *117*, 1759.
[40] K. Awasthi, T. Nakabayashi, N. Ohta, *J. Phys. Chem. B* **2012**, *116*, 11159.

AUTHOR BIOGRAPHIES

Sudhakar Narra received his doctoral degree in Physical Chemistry from the Department of Applied Chemistry, National Chiao Tung University in the year 2014 under the supervision of Prof. Shinsuke Shigeto. Currently, he is working as a

postdoctoral researcher at the same university. His research interests are structural studies, dynamics, and electric field effects on functional materials using ultrafast optical spectroscopy.

Shuo-En Tsai received bachelor's degree in science for chemistry from National Cheng Kung University in the year 2019. Now he is pursuing his master's degree in chemistry from the department of applied chemistry in National Yang Ming Chia Tung University. His research mainly focuses on the electric field effects on the polymers related to organic solar cells.

Kamlesh Awasthi received his Ph. D. in Material Science from Hokkaido University, Japan, in 2009. From April 2009 to March 2013, he worked as a postdoctoral research fellow at Research Institute for Electronic Science, Hokkaido University, Japan. From April 2013 to March 2015, he worked as a Specially Appointed Assistant Professor at Hokkaido University, Japan. In 2015, he joined National Chiao Tung University (now National Yang Ming Chiao Tung University), Taiwan, as an Assistant Research Fellow. His research interests are based on living cells, tissues, and semiconductor optoelectronics, photovoltaic and material science, photoelectrics, and photobioelectrics.

Shailesh Rana is currently working as a PhD student in the Department of Applied Chemistry, National Yang Ming Chiao Tung University, Taiwan, under the joint supervision of Prof. Eric Wei-Guang Diau and Prof. Nobuhiro Ohta. He obtained his MSc degree in physics from Kumaun University, India. His research work includes thin film fabrication, electric field effect on optical properties, and device physics of perovskite materials.

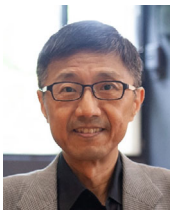

Eric Wei-Guang Diau started his research in 2001 in the Department of Applied Chemistry and Science of Molecular Science, National Chiao Tung University (NCTU), Taiwan. His current research is focusing on the developments of novel perovskites and functional materials for applications in photovoltaics, photocatalysis, light emitting diode, display, and so on. He received "Sun Yat Sen Academic Award" in 2014, "MOST Outstanding Research Award" in 2018, and "17th Hsu Yu-Ziang Science Paper Award" in 2019. He has published over 210 peer-reviewed papers with H-index 65. He is currently Distinguished Professor at Department of Applied Chemistry of National Yang Ming Chiao Tung University (NYCU), Taiwan.

Nobuhiro Ohta is currently a Chair Professor at Department of Applied Chemistry/Institute of Molecular Science and Center for Emergent Functional Matter Science, National Yang Ming Chiao Tung University (NYCU), Taiwan, and Professor Emeritus at Hokkaido University, Japan. Before joining National Chiao Tung University (now NYCU), he was a Professor at Research Institute for Electronic Science, Hokkaido University, Japan. His research interests are electric field effects on structure, dynamics and function of molecules, optoelectronic materials, and live cells.

SUPPORTING INFORMATION

Additional supporting information may be found in the online version of the article at the publisher's website.

How to cite this article: S. Narra, S.-E. Tsai, K. Awasthi, S. Rana, E. W.-G. Diau, N. Ohta, *J. Chin. Chem. Soc.* **2022**, *69*(1), 140. https://doi.org/10.1002/jccs.202100267